







Impact of increasing carbon dioxide on dinitrogen and carbon fixation rates under oligotrophic conditions and simulated upwelling

Arvind Singh ^{1,2*} Lennart T. Bach ^{1,3} Carolin R. Löscher ^{1,4} Allanah J. Paul ¹ Narendra Ojha ²
Ulf Riebesell ¹

¹GEOMAR Helmholtz Center for Ocean Research Kiel, Kiel, Germany

²Physical Research Laboratory, Ahmedabad, India

³Institute for Marine and Antarctic Studies, University of Tasmania, Hobart, Australia

⁴Department of Biology, Nordcee, Danish Institute for Advanced Study, University of Southern Denmark, Odense, Denmark

Abstract

Dinitrogen (N₂) fixation is a major source of bioavailable nitrogen to oligotrophic ocean communities. Yet, we have limited understanding how ongoing climate change could alter N₂ fixation. Most of our understanding is based on short-term laboratory experiments conducted on individual N₂-fixing species whereas community-level approaches are rare. In this longer-term in situ mesocosm study, we aimed to improve our understanding on the role of rising atmospheric carbon dioxide (CO₂) and simulated deep water upwelling on N₂ and carbon (C) fixation rates in a natural oligotrophic plankton community. We deployed nine mesocosms in the subtropical North Atlantic Ocean and enriched seven of these with CO₂ to yield a range of treatments (partial pressure of CO₂, *p*CO₂ = 352–1025 μatm). We measured rates of N₂ and C fixation in both light and dark incubations over the 55-day study period. High *p*CO₂ negatively impacted light and dark N₂ fixation rates in the oligotrophic phase before simulated upwelling, while the effect reversed in the light N₂ fixation rates in the bloom decay phase after added nutrients were consumed. Dust deposition and simulated upwelling of nutrient-rich deep water increased N₂ fixation rates and *nifH* gene abundances of selected clades including the unicellular diazotrophic cyanobacterium clade UCYN-B. Elevated *p*CO₂ increased C fixation rates in the decay phase. We conclude that elevated *p*CO₂ and pulses of upwelling have pronounced effects on diazotrophy and primary producers, and upwelling and dust deposition modify the *p*CO₂ effect in natural assemblages.

The capacity of the marine microbes to fix atmospheric carbon dioxide (CO₂) is largely governed by the availability of bioavailable nitrogen, such as nitrate (NO₃[−]) and ammonium (NH₄⁺), in the sunlit ocean (Falkowski 1997). Biological dinitrogen (N₂) fixation, although an energetically expensive process, is a major source of bioavailable nitrogen to marine biota in oligotrophic waters in equatorial, tropical, and subtropical regions (Zhang et al. 2020). Despite recognizing the role of

anthropogenic activities on the nitrogen cycle, the influence of ongoing climatic changes on N₂ fixation is insufficiently understood (Jickells et al. 2017; Zehr and Capone 2020).

Partial pressure of CO₂ (*p*CO₂) in the atmosphere has increased from nearly 280 μmol mol^{−1} in 1750 to 416 μmol mol^{−1} in 2021 (Keeling and Keeling 2017). Under the high CO₂ emission scenario RCP8.5, *p*CO₂ may rise above 1000 μmol mol^{−1} by 2100 (Moss et al. 2010). The ocean is one of the largest sinks of CO₂ and removes around 30% of the anthropogenic carbon (C) added to the atmosphere (Gruber et al. 2019). Consequential rise in oceanic *p*CO₂ is considered a threat to marine ecosystems (Doney et al. 2020). While marine scientists have studied its impact on many ocean phytoplankton species (e.g., Riebesell 2004), its role on community level N₂ fixation remains less well understood (Hutchins and Fu 2017). Previous studies on open ocean N₂ fixers were carried out mainly on *Trichodesmium* and *Crocospaera* (UCYN-B), two common diazotrophic species in the ocean, in monoclonal culture experiments (e.g., Hutchins et al., 2007; Fu et al., 2008; Wannicke et al., 2018). Those studies underscored the mixed physiological response on nitrogenase

*Correspondence: arvinds@prl.res.in

This is an open access article under the terms of the Creative Commons Attribution License, which permits use, distribution and reproduction in any medium, provided the original work is properly cited.

Additional Supporting Information may be found in the online version of this article.

Author Contribution Statement: Arvind Singh and Allanah J. Paul designed incubation experiments, while Lennart T. Bach and Ulf Riebesell designed the mesocosm experiment along with the KOSMOS team. Carolin R. Löscher did the molecular analysis. Narendra Ojha analyzed model AOD data. Arvind Singh wrote the manuscript with inputs from all the coauthors.

activity in individual species to elevated $p\text{CO}_2$. However, laboratory experiments do not consider ecological interactions, e. g., competition for nutrients among diazotrophs and other phytoplankton, which result from both direct and indirect effects of high $p\text{CO}_2$. Moreover, the most widely distributed cyanobacterial diazotroph, UCYN-A, has not been yet brought into culture (Zehr et al. 2008; Tang et al. 2019). As such, culture studies are not fully representative as they overlook an important part of the diazotrophic community and their interactions in the environment. To address these limitations and gain insights into a natural community's response to high $p\text{CO}_2$, we have sub-sampled an in situ mesocosm experiment with eight different $p\text{CO}_2$ levels ranging from the present day atmospheric value to levels projected for the end of this century under selected CO_2 emission scenarios (Bindoff et al. 2019).

Most autotrophic organisms, including diazotrophs possess CO_2 concentrating mechanisms, which promote C fixation by accumulating CO_2 around the CO_2 -fixing enzyme RuBisCO (Badger et al. 2005). Thus, in a high $p\text{CO}_2$ ocean, these marine diazotrophs may be able to redirect their energy/resources to fix N_2 . This has stimulated the hypothesis that overall N_2 fixation rates will increase at higher $p\text{CO}_2$ levels (Barcelos e Ramos et al. 2007; Hutchins et al. 2007). However, some unicellular diazotrophs such as UCYN-A lack the oxygen-evolving photosystem II and the metabolic ability to fix inorganic C (Zehr et al. 2008). Hence, these species may not directly benefit from high CO_2 . Besides, these unicellular diazotrophs are often found in symbiosis with unicellular eukaryotic algae (Thompson and Zehr 2013). Unicellular diazotrophic cyanobacterium clade UCYN-A and its symbiotic algae transfer nitrogen and C to each other (Thompson et al. 2012), thus high CO_2 may indirectly benefit them. Unicellular diazotrophic cyanobacterium clade UCYN-B fix C themselves, so they could potentially benefit directly from elevated CO_2 (Mohr et al. 2010b; Rabouille et al. 2017). This study was aimed to test the hypothesis that N_2 fixation will increase with increasing $p\text{CO}_2$ levels in the natural environment.

In addition to altered $p\text{CO}_2$ levels in the future ocean, upwelling is predicted to intensify in many oceanic regimes (Narayan et al. 2010; Wang et al. 2015). The Canary Current System is regularly perturbed by natural upwelling via eddies or filaments (Santana-Falcón et al. 2020). Upwelling intensification may impact nutrient cycling in such regimes with a potential enrichment of surface waters with nutrients and thereby increasing primary productivity (Aure et al. 2007). For example, filament structures such as Cape Ghir in the Canary Current Upwelling System, which export 2–3 times more C compared to other filaments (Sangrà et al. 2015), might fix even more C with enhanced upwelling (Xiu et al. 2018). It is unclear what impact upwelling of nutrient-rich water has on surface N_2 fixation rates.

Growth of diazotrophy is limited by iron (Fe) and phosphorus nutrients (Mills et al. 2004). Upwelling and dust deposition are two important sources of such nutrients in the sunlit

ocean. Rates of N_2 fixation associated with unicellular diazotrophs can be doubled due to dust deposition events in the Canary Islands (Benavides et al. 2013). Non-diazotrophic primary producers (e.g., diatoms) outcompete diazotrophs with regard to direct nutrient uptake during upwelling (Mills and Arrigo 2010). In addition, the nitrate: phosphate (NO_3^- : PO_4^{3-}) ratio in surface waters has been proposed to play a major role for nutrient cycling and primary production (Tyrrell 1999). Sub-surface waters, when upwelled, have potential to change surface water nutrient stoichiometry (Franz et al. 2012), and, in turn, can influence N_2 fixation rates. From the biogeochemical modeling point of view, the mathematical expression for excess phosphorus, i.e., $P^* = ([\text{PO}_4^{3-}] - [\text{NO}_3^-]/16)$, which is based on the Redfield ratio, is useful for estimating the distribution of N_2 fixation rates where atmospheric dust deposition is sufficient (Deutsch et al. 2007; Knapp et al. 2016). Sub-surface water in the Atlantic is generally depleted in PO_4^{3-} (negative P^*) compared to NO_3^- (Lomas et al. 2010; Singh et al. 2015). Introduction of high NO_3^- and low PO_4^{3-} water to a surface plankton community might inhibit N_2 fixation rates (Knapp et al. 2012). Hence, we tested a second hypothesis, which was that the addition of deep water (simulating future upwelling events) will decrease N_2 fixation rates due to higher bioavailable inorganic nitrogen concentrations.

Methods

Mesocosm set-up

A detailed methodology on the mesocosm study set-up and carbonate chemistry manipulation is provided in Taucher et al. (2017) but we give a brief account here on the mesocosm setup as well as a detailed explanation of incubations carried out for analysis of C and N_2 fixation rates. Nine “Kiel Off-Shore Mesocosms for Ocean Simulations” (KOSMOS; Riebesell et al. 2013) were deployed in the northern part of Gando Bay ($27^\circ 56' \text{ N}$, $15^\circ 22' \text{ W}$, eastern North Atlantic) in Gran Canaria at a water depth of $\sim 20\text{--}25 \text{ m}$ on 23 September 2014. Each mesocosm contained around 35,000 L ($31.6\text{--}37.8 \text{ m}^3$) seawater. Two mesocosms were set up as controls (369 and 352 $\mu\text{atm } p\text{CO}_2$, respectively) and therefore not treated with CO_2 additions, while others were enriched with CO_2 saturated water with a gradient of seven individual treatments (448, 563, 668, 716, 887, 976, and 1025 $\mu\text{atm } p\text{CO}_2$ averaged over the experimental duration, distributed randomly in seven mesocosms). The first CO_2 manipulation was done stepwise at the beginning of the study during 1–6 October 2014 (day 0 is counted from 1 October) to establish the treatments and allow some time for acclimation, followed by manipulations on days 21 and 38 to maintain targeted $p\text{CO}_2$ levels. Deep water was collected from 650 m depth at a location ($27^\circ 57' \text{ N}$, $15^\circ 18' \text{ W}$) about 4 nautical miles north-east from the study site where the water depth was about 1000 m. We simulated upwelling by replacing $\sim 20\%$ of water in each mesocosm with the collected

deep water during the night from day 24 to 25. Mesocosms were sampled over 0–13 m depth using an integrated water sampler (HydroBIOS, Kiel) before noon on each sampling day.

Carbonate chemistry analyses, nutrient measurements and aerosol optical depth estimates

Samples for dissolved inorganic carbon and total alkalinity were gently filtered (0.2 μm pore size) using a peristaltic pump and measured on the same day. Dissolved inorganic carbon concentrations were determined by infrared absorption using a LI-COR LI-7000 on an AIRICA system (MARIANDA, Kiel) with an overall precision better than 5 $\mu\text{mol kg}^{-1}$. Total alkalinity was measured by potentiometric titration using a Metrohm 862 Compact Titrator and a 907 Titrando unit following Dickson et al. (2003). The estimates of $p\text{CO}_2$ values were based on measured total alkalinity, dissolved inorganic carbon, silicate, and PO_4^{3-} concentrations as well as measured temperature and salinity using CO2SYS (Pierrot et al. 2011) and carbonate chemistry constants by Lueker et al. (2000). Nutrient samples were collected in acid-cleaned (10% HCl) bottles (PETG), filtered (0.45 μm pore size filter, cellulose acetate filters, Whatman) immediately upon arrival of samples in the laboratory, and analyzed on the same day. Concentrations of NO_x^- ($\text{NO}_3^- + \text{NO}_2^-$), $\text{Si}(\text{OH})_4$, and PO_4^{3-} were measured with a SEAL Analytical QuAAtro AutoAnalyzer following Hansen and Koroleff (2007). Precision (detection limit) of nutrients (based on standard deviation of triplicates) was $\pm 0.007 \mu\text{M}$ (0.03 μM) for NO_x^- , $\pm 0.003 \mu\text{M}$ (0.008 μM) for PO_4^{3-} and $\pm 0.011 \mu\text{M}$ (0.05 μM) for $\text{Si}(\text{OH})_4$.

Daily total and dust aerosol optical depth (AOD) at 550 nm over the study region (27°–28° N, 15°–16° W) has been derived from the Copernicus Atmosphere Monitoring Service (CAMS) model reanalysis (Inness et al. 2019). The CAMS reanalysis are global fields of atmospheric composition developed by the European Centre for Medium-Range Weather Forecasts (ECMWF). The CAMS model system assimilates a suite of satellite-based observations related to trace gases and aerosols with the Integrated Forecasting System. The CAMS reanalysis has improved spatial and temporal resolutions (80 km, 3-hourly), and this model has been shown to have smaller biases when compared with independent observational datasets (Inness et al. 2019).

Carbon and nitrogen fixation experiments

We did 14 dark incubations and 11 light incubations for C and N_2 fixation rate measurements without replication for each $p\text{CO}_2$ level on different days from day – 3 (28 September 2014, 3 days before the first CO_2 enrichment was done in the mesocosms) to day 55 (25 November 2014). We started light incubations from day 11. During each morning of the experimental day, water samples from the nine mesocosms and surrounding Atlantic water (for reference) were collected over 0–13 m depth using the integrated water sampler and transferred into 2.8 L polycarbonate bottles (Nalgene, Thermo Fisher

Scientific, Waltham, MA) on board the sampling boats. Polycarbonate bottles were stored in a cool box to control temperature and to block sunlight until return to the on-shore laboratory.

Due to the low nutrient concentrations, surface Atlantic water was used to prepare dissolved $^{15}\text{N}_2$ solution (98% atom% ^{15}N , Lot No. I-18404, Cambridge Isotope Laboratories, MA) on each sampling day following a method modified from Mohr et al. (2010a). Dissolution of the $^{15}\text{N}_2$ gas was achieved by ~ 30 min of gentle slapping of the enriched gas bubble in a gas sampling bag (Tedlar bag with single polypropylene fitting) with a ruler. Each sample bottle was mixed gently by rotating around 10 times before 50 mL of water was removed to make space for the dissolved $^{15}\text{N}_2$ enriched seawater. Subsequently, 50 mL of this dissolved labeled $^{15}\text{N}_2$ tracer water was added to each polycarbonate bottle to achieve a final ^{15}N enrichment of 2.35 atom %. Additionally, 1 mL (0.2 M concentration) of labeled $\text{NaH}^{13}\text{CO}_3$ (99%, Cambridge Isotope Laboratories, MA) dissolved in deionized water was added to the same 2.8 L bottles for primary production rate measurements (C fixation rates). By mistake, we added 2 mL of the same concentration of $\text{NaH}^{13}\text{CO}_3$ during the days 25 to 37 for C fixation rates. Carbon isotopic (^{13}C) enrichment was estimated for each mesocosm based on the ambient dissolved inorganic carbon concentrations as reported by Taucher et al. (2017). The ^{13}C enrichment varied from 4.06 to 7.08 atom % (higher enrichment were during the days 25 to 37). After addition of both the tracers, bottles were closed and gently rotated to mix the water.

For light incubations, sample bottles were placed in an incubator covered with 25% transmittance filter sheet (Blue Lagoon, LEE filters) for 24 h at the Spanish Bank of Algae, next to the land-based facilities of the Plataforma Oceánica de Canarias (PLOCAN). For the dark incubations, sample bottles were placed in a fully closed and covered cemented tank inside a laboratory at PLOCAN for 24 h in running seawater. Running seawater was used to maintain in situ temperature in both the light and dark incubations, which ranged from 26°C initially to 21.5°C towards the end of the study in November. After 24 h of incubation, a subsample of seawater from each incubation bottle (volume: 0.5–2.8 L, depending on sample biomass) was filtered onto pre-combusted (450°C, 5 h) 25 mm diameter glass fiber filters using vacuum filtration (< 200 mbar pressure). We used 0.7 μm pore size filters (GF/F, Whatman, UK) for light incubations and 0.3 μm pore size filters (GF75, Advantec, Toyo Roshi Kaisha Ltd., Japan) for dark incubations, in order to capture smaller heterotrophic diazotrophs in dark incubations that can pass through the 0.7 μm GF/F (Bombar et al. 2018). All filtrations were completed within 2 h. Filters were dried at 50°C for 24 h and stored in cryogenic vials until mass spectrometric analysis. Samples for background isotope abundances in particulate organic matter were collected from the mesocosms and filtered onto GF filters as described for the incubations.

For isotope analysis, the filters were stored over concentrated (36%) HCl for 4 h in a desiccator so that the acidic fumes removed carbonates present. Filters were then dried overnight in an oven at 50°C and later pelletized in tin cups. Samples were analyzed for particulate organic carbon (POC) and nitrogen (PON) and their isotopic composition ($\delta^{15}\text{N}$ and $\delta^{13}\text{C}$) using an elemental analyzer coupled to a ConFlo II and a Finnigan Delta^{plus} isotope ratio mass spectrometer (IRMS) at GEOMAR, Kiel. International Atomic Energy Agency (IAEA) standard materials (acetanilide, caffeine) were used for mass and isotope calibration of C and N (standard deviation < 0.2‰ $\delta^{15}\text{N}$ and $\delta^{13}\text{C}$). Nitrogen fixation rates were calculated following Montoya et al. (1996):

$$\text{N}_2 \text{ fixation} = \left(\frac{1}{t} \right) \left(\frac{A_{\text{PN}_f} - A_{\text{PN}_0}}{A_{\text{N}_2} - A_{\text{PN}_0}} \right) [\text{PON}_f]$$

where t = incubation time, A_{PN_f} = ^{15}N atom% in PON at the end of incubation, A_{PN_0} = ^{15}N atom% in PON at the start of the incubation, A_{N_2} = ^{15}N enrichment in the dissolved form after the tracer addition at the start of the incubation, and PON_f refers to particulate organic nitrogen concentration at the end of the incubation. In the above equation, all the terms are measured except A_{N_2} , which is defined as:

$$A_{\text{N}_2} = \left(\frac{^{15}\text{N}_{\text{tracer}} \times \text{tracer concentration} + ^{15}\text{N}_{\text{natural}} \times \text{natural concentration}}{\text{tracer concentration} + \text{natural concentration}} \right)$$

The natural concentration of dissolved N₂ for a given temperature and salinity was calculated using the table given in Weiss (1970). Carbon fixation rates were calculated similar to N₂ fixation rates following Slawyk et al. (1977). Taking into account all the sources of uncertainty (detection limits for POC and PON are 15 and 5 µg, respectively; precisions of $\delta^{13}\text{C}$ and $\delta^{15}\text{N}$ to be 0.2), our detection limits for C and N₂ fixation rates were 0.12 and 0.05 nM N h⁻¹, respectively. Most of the samples for day 35 (belonging to dark incubations for nitrogen analysis only) were lost due to the technical issues with IRMS.

Molecular methods

Seawater samples were taken directly from the mesocosms on days 1, 3, 19, 25, 28, 35, 41, and 53 of the experiment runtime, in volumes between 1 and 2 L. The water was filtered on 0.2 µm pore size membrane filters (Millipore) and kept at -80°C until further analysis. Nucleic acids were extracted using the Qiagen AllPrep DNA/RNA kit with modifications as described in Loescher et al. (2014). After spectrophotometric quality checks (NanoDrop), a PCR for the key functional marker gene for N₂ fixation, *nifH* was performed following the protocol of Zani et al. (2000). The *nifH* PCR products were pooled, Topo TA cloned (Thermo Fisher Scientific) and Sanger-sequenced as a commercially available service, in order to identify major present diazotrophic clades. We performed qPCR analyses for filamentous

cyanobacteria, UCYN-A, -B, -C, gammaproteobacteria of the AO and PO types, and the Het I and II clades (Langlois et al. 2005; Foster and Zehr 2006). The qPCRs were performed as described in Loescher et al. (2014) against plasmids containing an environmental copy of the target gene (standards obtained from Langlois et al. [2008]), in technical duplicates on a Biorad qPCR cycler. In addition, we enumerated *Trichodesmium* colonies using a microscope.

Statistical analysis

We analyzed the *nifH* gene abundances, C and N₂ fixation rates for three different experimental phases separately: (1) the oligotrophic phase after CO₂ addition until day 23, (2) the phytoplankton bloom (growth) phase after simulated upwelling between day 25 and day 35, and (3) the post-bloom (decay) phase from day 37 until the end of the study. Phases are delineated based on the concentrations of nutrients and chlorophyll—oligotrophic (low nutrients), growth (increase in chlorophyll due to deep water addition) and decay phase (decline of chlorophyll; Taucher et al. 2017). As done previously in such mesocosm experiments (Paul et al. 2015), a pCO₂ gradient was chosen for the reasons described in Havenhand et al. (2010). We did linear regression analyses (significant at $p < 0.05$) to determine the effect of pCO₂ on C and N₂ fixation rates for each phase. Variables for each phase were averaged and plotted against the average pCO₂ in each mesocosm in the corresponding phases. All the data points after day 0 are included in the analysis. Units for normalized rates changed to h⁻¹ (e.g., nM N h⁻¹/[PON] = h⁻¹ for N₂ fixation). Since rates in h⁻¹ were low, we report the rates in day⁻¹.

Results

Variation in aerosol optical depth and inorganic nutrients

Variations in the total and dust AOD suggested three dust events over the study region during the experimental duration (Fig. 1). Initiation of these dust events were on days 1, 18 and 31. The second dust event, which started before the growth phase, lasted longer (11 days) as compared to other events. The second dust event was recognized as a Calima event. Calima events are those events in the Canaries which are associated with hot, dry and thick dust layers in the lower atmosphere.

Environmental conditions changed from oligotrophic to eutrophic phase in the mesocosms after deep water addition (Fig. 2). Concentrations of NO_x⁻ were below 0.2 µM until day 23, thereafter peaked around 3.1 µM throughout the mesocosms following the deep water addition. Concentrations of PO₄³⁻ were close to detection limit (0.05 µM) before the deep water addition but increased up to 0.2 µM after addition. Unlike NO_x⁻ and PO₄³⁻, SiO₄ concentrations were relatively higher (0.5 µM) at the start of the experiment and decreased until day 23, followed by an increase of up to 2 µM after deep

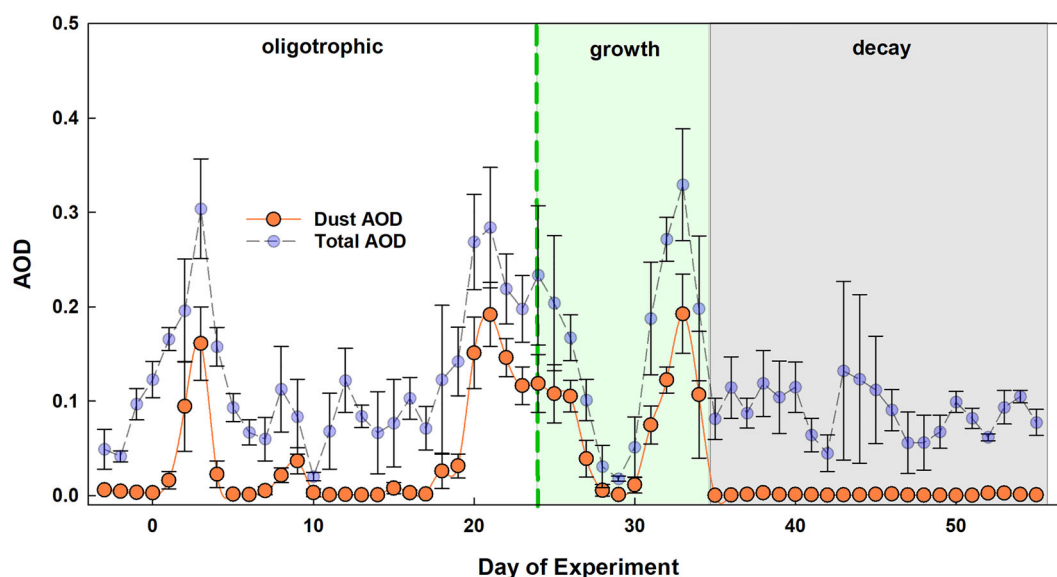


Fig 1. Variation in the daily means of dust aerosol optical depth (AOD) and total AOD over the study area. Error bars represent standard deviation (1σ) of 3-hourly values. Day 0 (1 October 2014) indicates the day of the first CO_2 manipulation, corresponding to the start of elevated $p\text{CO}_2$ treatments. The dashed green line represents the time of deep water addition, which was done on the night of day 24. White, green, and gray-shaded areas represent oligotrophic, growth, and decay phases, respectively.

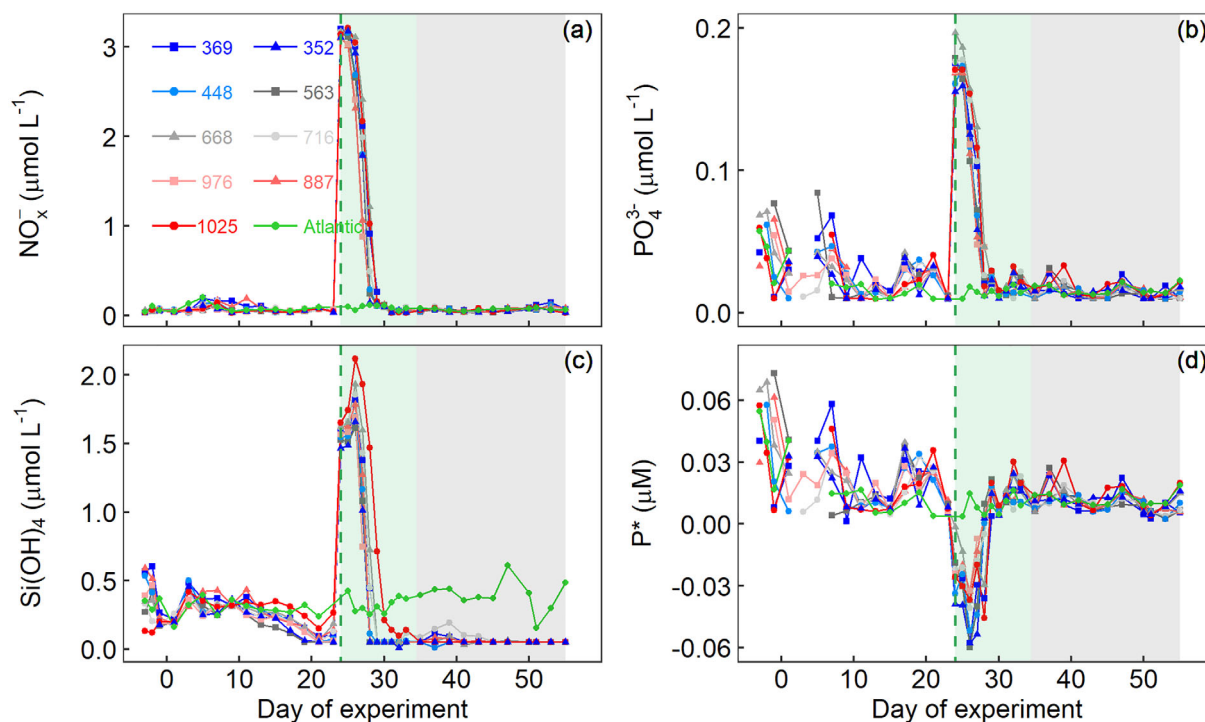


Fig 2. (a) NO_x^- , (b) PO_4^{3-} , (c) Si(OH)_4 concentrations, and (d) P^* values ($P^* = [\text{PO}_4^{3-}] - [\text{NO}_3^- + \text{NO}_2^-]/16$). Day 0 (1 October 2014) indicates the day of the first CO_2 manipulation, corresponding to the start of elevated $p\text{CO}_2$ treatments. Legend numbers indicate $p\text{CO}_2$ (μatm) averaged over the study period. The dashed green line represents the time of deep water addition, which was done on the night of day 24. White, green, and gray-shaded areas represent oligotrophic, growth, and decay phases, respectively.

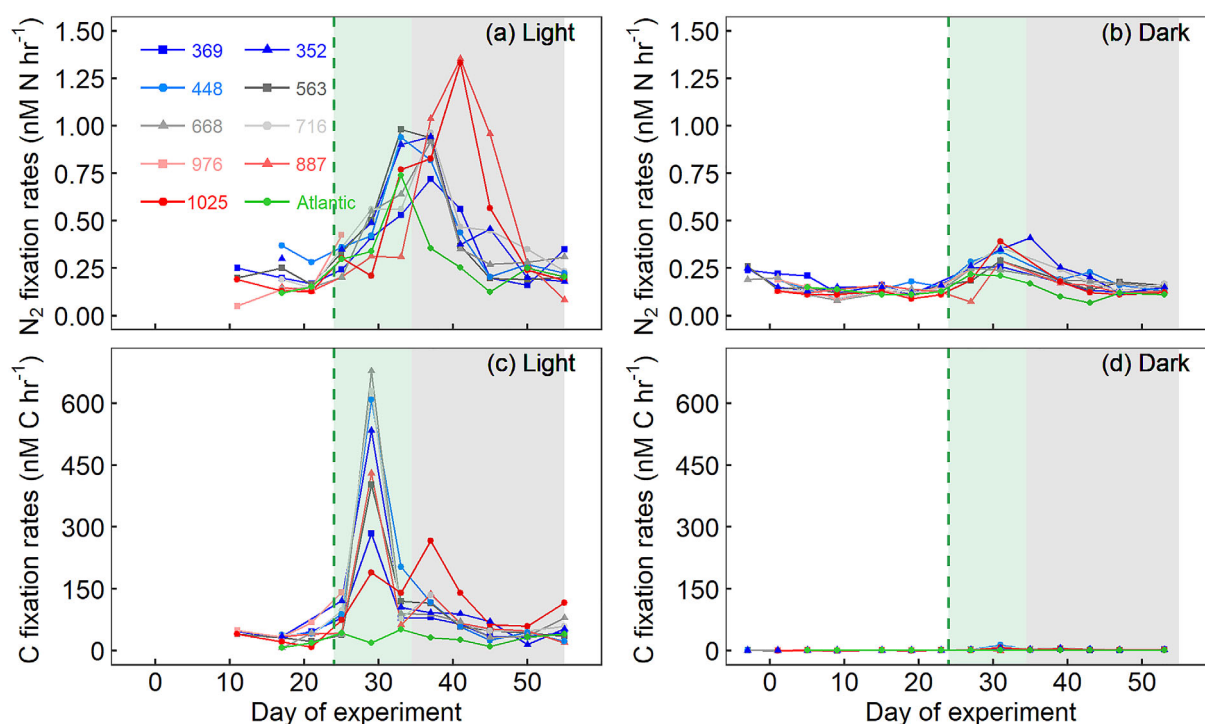


Fig 3. Daily variation in volumetric (a) phototrophic (incubation conducted in light) N_2 fixation rates, (b) dark N_2 fixation rates (incubation conducted in dark), (c) phototrophic C fixation rates (incubation conducted in light), and (d) dark C fixation rates (incubation conducted in dark). Legend numbers and colors are as described for Fig. 2.

water addition. All nutrients reached their previous concentration levels in <4 days after deep water addition, suggesting rapid and almost complete assimilation of nutrients added through deep water. Concentrations of NO_x^- and PO_4^{3-} were 16.71 and 1.05 μM , respectively, in the deep water, i.e., having a slightly positive P^* value (0.09 μM). Estimates of P^* in the mesocosms suggested that PO_4^{3-} was in excess until the deep water addition, and decreased thereafter due to possible preferential consumption of PO_4^{3-} in the first part of growth phase. Values of P^* turned positive again as soon as the nutrients from the deep water addition were consumed (day 29).

Influence of rising carbon dioxide on carbon and nitrogen fixation rates

Phototrophic N_2 fixation rates from the light incubations varied between 0.05 and 1.35 nM N h^{-1} (mean \pm standard deviation, i.e., $\mu \pm \sigma = 0.40 \pm 0.28 \text{ nM N h}^{-1}$, number of data points for all the mesocosms for all the sampling days, $n = 87$). Rates were below average in the oligotrophic phase, while they increased gradually during the growth phase and attained their peak during the decay phase in most mesocosms (Fig. 3a). Higher rates were associated with high $p\text{CO}_2$ mesocosms during the decay phase. Interestingly, rates in the surrounding (Atlantic) water also increased during the growth phase but decreased to the oligotrophic phase level in the decay phase. Regression

analysis suggested a negative effect of $p\text{CO}_2$ on N_2 fixation rates in the oligotrophic phase, whereas it had a positive effect in the decay phase (Table 1). The CO_2 effect was negative in the growth phase as well but it was statistically insignificant.

Dark N_2 fixation rates were lower compared to phototrophic N_2 fixation rates (Fig. 3a, b), and varied between 0.07 and 0.41 nM N h^{-1} ($\mu \pm \sigma = 0.17 \pm 0.07 \text{ nM N h}^{-1}$). Like phototrophic N_2 fixation rates, regression analysis suggested that dark N_2 fixation rates were negatively influenced by $p\text{CO}_2$ levels during the oligotrophic phase (Table 1). The levels of $p\text{CO}_2$ did not change dark N_2 fixation rates during growth and decay phases.

Phototrophic C fixation rates (from the light incubation) varied between 7 and 678 nM C h^{-1} ($\mu \pm \sigma = 96 \pm 129 \text{ nM C h}^{-1}$). Like N_2 fixation rates, there was a positive effect of $p\text{CO}_2$ levels on C fixation rates during the decay phase (Table 1). Carbon fixation rates from dark incubations (dark C fixation) remained close to their detection limits (Fig. 3d) and varied between 0 and 14 nM C h^{-1} ($\mu \pm \sigma = 2 \pm 2 \text{ nM C h}^{-1}$).

We extended similar regression analysis on C and N_2 fixation rates normalized by corresponding POC and PON concentrations, respectively. Phase-wise patterns of normalized rates were somewhat similar to volumetric rates (Fig. 4) but the effect of $p\text{CO}_2$ on C (phototrophic) and N_2 fixation rates was not statistically significant (Table 1).

Table 1. Summary of linear regression of $p\text{CO}_2$ on different variables for each phase. The variables and $p\text{CO}_2$ were averaged for each phase. Significant effects ($p < 0.05$) are listed in bold. Phase I = oligotrophic, phase II = bloom and phase III = decay. Total degrees of freedom, $df = 8$ for the first phase, and $df = 7$ for second and third phase as we lost one mesocosm having average $p\text{CO}_2 = 976 \mu\text{atm}$ after the first phase.

Phase	Variable*	<i>p</i>	<i>r</i>	<i>F</i>	Variable (normalized)	<i>p</i>	<i>R</i>	<i>F</i>
I	N_2 fixation (light)	0.01	−0.77	10.27	N_2 fixation (light)	0.07	−0.62	4.46
II		0.15	−0.56	2.69		0.19	−0.52	2.33
III		0.02	0.78	9.05		0.16	0.54	2.53
I	N_2 fixation (dark)	0.001	−0.91	34.47	N_2 fixation (dark)	0.11	−0.56	3.28
II		0.85	−0.35	0.39		0.49	−0.28	0.53
III		0.45	−0.31	0.65		0.20	−0.51	2.51
I	C fixation (light)	0.63	−0.19	0.26	C fixation (light)	0.73	−0.14	0.13
II		0.28	−0.44	1.44		0.32	−0.41	1.20
III		0.05	0.70	5.91		0.65	0.19	0.22

*Statistics for C fixation (dark) rates is not presented as these rates were close to their analytical uncertainties.

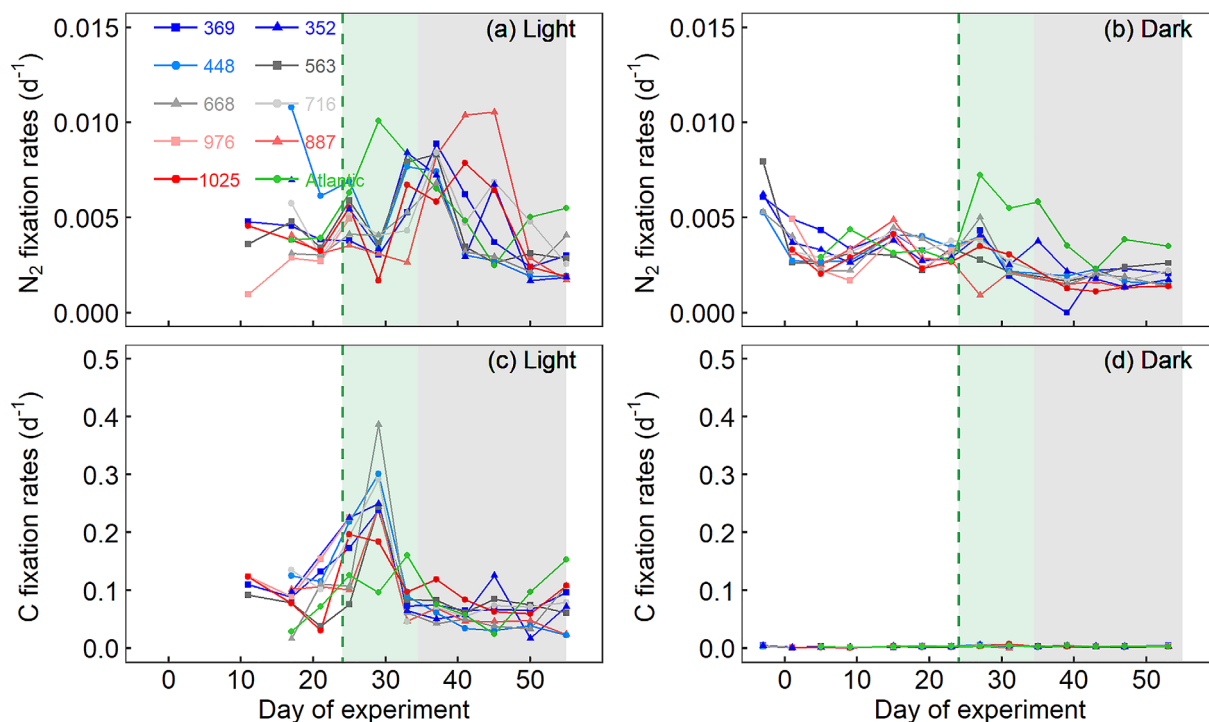


Fig 4. Daily variation in concentration normalized (a) phototrophic (incubation conducted in light) N_2 fixation rates, (b) N_2 fixation rates (incubation conducted in dark), (c) C fixation rates (incubation conducted in light), and (d) C fixation rates (incubation conducted in dark). Legend numbers and colors are as described for Fig. 2.

Carbon and nitrogen fixation rates following deep water additions

The simulated upwelling event had a profound impact on volumetric C and N_2 fixation rates from the light incubations (Fig. 3). Phototrophic N_2 fixation rates increased gradually following the addition of nutrient-rich deep water and dust deposition, and reached up to five times the initial rates after a week in all the mesocosms (Fig. 3a). Rates continued to increase in the two mesocosms with the highest CO_2

levels until day 40 (16 d after deep water addition). Likewise, dark N_2 fixation rates increased following deep water addition but these were barely twice the initial rates (Fig. 3b). The magnitude of the increase in dark N_2 fixation rates were similar in different CO_2 levels. Light C fixation rates increased immediately after simulated upwelling, peaking four days later and declining thereafter (Fig. 3c). There was no such observable change in the dark C fixation rates (Fig. 3d).

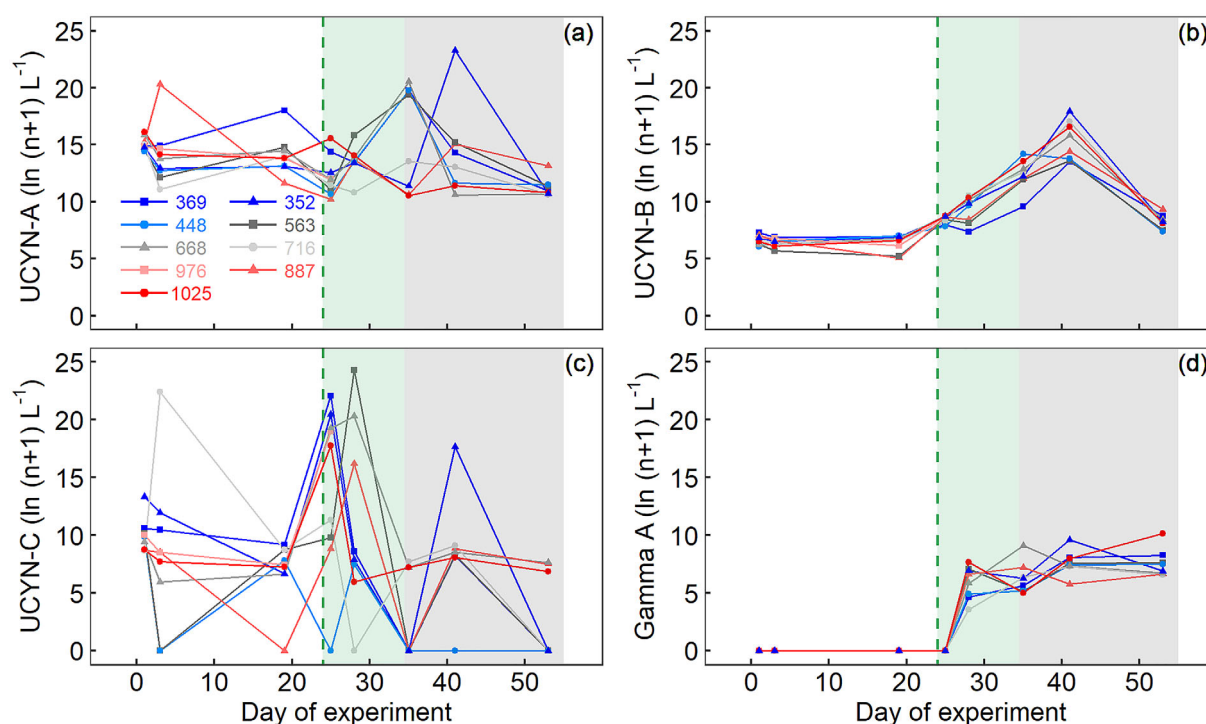


Fig 5. Daily variation in *nifH* gene abundances (on log scale, n represent copies of DNA detected) for (a) UCYN-A, (b) UCYN-B, (c) UCYN-C, and (d) Gamma A proteobacteria. Only AO (Atlantic Ocean) type gammaproteobacteria is shown here as PO (Pacific Ocean) type was mostly undetected throughout the experiment). Legend numbers and colors are as described for Fig. 2.

However, when the rates were normalized with their respective elemental concentrations, the impact of the simulated upwelling is less discernible on N_2 fixation (both light and dark) rates (Fig. 4a,b). Normalized phototrophic C fixation rates were slightly higher, whereas normalized dark C fixation rates remain unchanged and close to detection limit after the deep water addition (Fig. 4c,d).

Composition of the diazotrophic community

We observed a diazotrophic community typical for the eastern subtropical North Atlantic, including filamentous, unicellular cyanobacteria, and gammaproteobacteria matching the Atlantic Ocean type (Fig. 5). None of the diazotroph clades (i.e., UCYN-A, -B, -C, gammaproteobacteria) were significantly (at $p < 0.05$) influenced by high $p\text{CO}_2$ in the different phases, so we have not listed the corresponding regression analysis. However, we observed a temporal increase in unicellular cyanobacteria of the UCYN-B clade, and to a lesser extent, of the gammaproteobacteria after deep water addition and dust pulse. *Trichodesmium* colonies (from microscopic observations) were never counted to be above 1 colony L^{-1} in any of the mesocosms and only detected in genetic analyses before deep water addition (data not shown).

Discussion

Variable carbon dioxide response dependent on nutrient concentrations and plankton bloom status

Our results suggest a variable effect of CO_2 on N_2 fixation rates. Under nutrient deplete conditions, both light and dark rates were negatively correlated with $p\text{CO}_2$, yet under decay conditions, the correlation was positive for light N_2 fixation rates. Overall the diazotrophic community was dominated by unicellular cyanobacteria, consistent with other observations in the eastern subtropical North Atlantic Ocean (Benavides et al. 2013). Nitrogen fixation by UCYN-A has been shown to be unaffected by high $p\text{CO}_2$ levels in a natural community of low dissolved Fe in oligotrophic conditions during short (5 d) acclimation experiments (Law et al. 2012). However, under double the modern $p\text{CO}_2$ levels and Fe replete conditions, rates of N_2 fixation by UCYN-B were reported to be enhanced by 80% in a culture experiment (Fu et al. 2008). A compilation of studies suggests that high $p\text{CO}_2$ affects N_2 fixation rates positively during Fe-replete conditions and negatively during Fe-depleted conditions (Table S1). We did not measure Fe in our samples, but our phototrophic N_2 fixation rates started increasing in all the treatments gradually after the deep water addition and dust deposition, both being important source of Fe. Rates in the waters from the Atlantic also started increasing around the same time. This might be due to the second

Calima event before the deep water addition that may have introduced large amounts of dust (iron), triggering N_2 fixation in the surrounding waters (Fig. 1). However, a rate increase in the mesocosms may not be only due to likely Fe inputs during the Calima event, as the increase in most mesocosms was somewhat higher (1.35 nM N h^{-1}) compared to the surrounding Atlantic waters (0.74 nM N h^{-1}). Rates peaked at 1.35 nM N h^{-1} , up to five times higher than in the oligotrophic phase in the highest $p\text{CO}_2$ treatments 17 days after the nutrient enrichment. This positive effect of high $p\text{CO}_2$ levels on N_2 fixation in the decay phase became insignificant in the biomass normalized rates (Fig. 4a, Table 1), suggesting that N_2 fixation rates are strongly dependent on the absolute planktonic community biomass present and to a lesser extent on the $p\text{CO}_2$ levels. Since diazotrophic biomass is a negligible fraction of planktonic community biomass in a natural community (Montoya et al. 2002), it could still be argued that the rates are community composition dependent.

In summary, N_2 fixation rates seem to be controlled by a complex interplay of different environmental conditions, including nutrient availability and stoichiometry. If our analysis is interpreted with respect to Fe-limited (during the oligotrophic phase) and Fe-rich (after deep water addition), then the observed CO_2 effects (negative during Fe-limitation, positive during Fe-replete conditions) are consistent with most of the laboratory/single-strain culture studies (Table S1). Hence, nutrient competition and other interactions in a natural plankton assemblage did not appear to modify the direct effects of elevated $p\text{CO}_2$ on N_2 fixation rates reported in culture studies.

Different response timing of nitrogen and carbon fixation to upwelling event

As per the *Trichodesmium* centric classical view, the first phase of the experiment would open up a niche for N_2 fixers, because of the oligotrophic (low bioavailable nitrogen) conditions (Capone et al. 1997). In the growth phase, increased NO_3^- from simulated upwelling would suppress phototrophic N_2 fixation (Holl and Montoya 2005). However, our observations (Fig. 3) are contrary to this classical view of high nitrogen (nutrient) concentrations inhibiting diazotrophic growth (Karl and Letelier 2008) as N_2 fixation rates and UCYN-B *nifH* copies gradually started increasing after nutrient-rich deep water addition and dust deposition. In fact, N_2 fixation is limited by Fe and PO_4^{3-} (Mills et al. 2004), and N_2 fixers are not strongly inhibited by inorganic nitrogen species such as NO_3^- (Fernandez et al. 2011; Loescher et al. 2014). In our study, we anticipate that biological nutrient uptake processes would have quickly increased because deep water contains ample amounts of nutrients for primary producers in this otherwise oligotrophic region. Hence slow growing N_2 fixers may have been outcompeted by rapidly growing phytoplankton such as diatoms as observed in the microscopy data (Taucher et al. 2018a) and in measured C fixation rates (light

incubations). Indeed, there was a quick build-up of biomass leading to a phytoplankton bloom, which declined long before diazotrophy peaked on day 41 (figs. 7 and 8 in Taucher et al., 2017). The phytoplankton bloom rapidly resulted into nitrogen limitation around day 29 (Taucher et al. 2018b), creating an amplified diazotrophic niche. We found high C fixation rates associated with a phytoplankton bloom on day 29, followed by an increase in N_2 fixation rates associated with concurrent high UCYN-B copies. Low NO_x^- , leftover PO_4^{3-} and Fe from the deep water and concurrent dust deposition might have contributed to N_2 fixation rates peaking on day 41 in high $p\text{CO}_2$ mesocosm. A recent meta-analysis consisting of published data on nine species, 18 different strains, and 18 experiments using natural plankton communities suggest an increase in N_2 fixation rates by $29 \pm 4\%$ under high $p\text{CO}_2$ scenarios (Wannicke et al., 2018). It has been noted that nutrient limitation (particularly by Fe) negates the positive effect of high $p\text{CO}_2$ on N_2 fixation (Wannicke et al. 2018). Integrating the results from all three phases of the present study, our data indeed indicate that N_2 fixation rates (in the light) are enhanced under elevated $p\text{CO}_2$ conditions if PO_4^{3-} is in excess and Fe is presumably available in higher concentrations. Overall, we suggest that the effects of CO_2 on N_2 fixation are regulated through changes in the plankton community structure and nutrient stoichiometry.

In addition to being the first in situ elevated $p\text{CO}_2$ mesocosm study in subtropical oligotrophic waters, this study is also the first large scale upwelling simulation primarily investigating its impact on C and N_2 fixation rates. Carbon fixation rates showed an increasing trend over 4 days upon upwelling simulation, followed by a decline, while N_2 fixation rates were still increasing. Concentrations of PO_4^{3-} were more than doubled from $0.07 \mu\text{M}$ before, to $\sim 0.2 \mu\text{M}$ after the deep water addition and P^* became negative ($-0.06 \mu\text{M}$). The increase in P^* to above 0 within a week of the deep water addition suggests that deep water NO_x^- was preferentially and rapidly consumed by non-diazotrophs (Mills and Arrigo 2010; Singh et al. 2017), which created an environment of excess PO_4^{3-} where diazotrophs could thrive as found in a PO_4^{3-} enriched mesocosm experiment (Bonnet et al. 2016). Over the course of the study, we indeed encountered a non-diazotrophic cyanobacterial bloom in the growth phase as corroborated in HPLC data (Taucher et al. 2018a). Non-diazotrophic cyanobacteria consume less PO_4^{3-} relative to NO_x^- compared to fast growing phytoplankton and N:P in their cells is higher than the Redfield ratio (Bertilsson et al. 2003; Singh et al. 2015). Estimates of P^* turned positive as soon as the deep water NO_x^- was consumed on day 28. This also coincided on day 29 with high N_2 fixation rates (average of all the light incubations $0.42 \pm 0.12 \text{ nM N h}^{-1}$). A delayed increase in N_2 fixation rates after deep water addition is likely because the diazotrophs are slow growing (Berman-Frank et al. 2001) and the niche had to first be established by non-diazotrophic organisms (Mills and Arrigo 2010; Singh et al. 2017). In summary, our results

suggest that the diazotrophic activity was stimulated potentially due to niche construction of excess PO_4^{3-} a few days after the addition of nutrient-rich deep water and dust deposition.

Rates of C fixation increased rapidly after deep water addition, indicating fast growing primary producers could take advantage of this nutrient input. In contrast, N_2 fixation rates peaked up to a week later. This lag likely reflects the slower growth rates of diazotrophic species in addition to construction of the niche by non-diazotrophic cyanobacteria. Additionally, this response lag could be due to the effect of elevated $p\text{CO}_2$ on the symbiotic relationship of unicellular diazotrophs with diatoms (Thompson and Zehr 2013). Higher N_2 fixation rates occurred in the high $p\text{CO}_2$ ($> 800 \mu\text{atm}$) mesocosms, in which ecological and biogeochemical processes were dominated by a bloom of the toxic microalga *Vicicitus globosus* (Riebesell et al. 2018). It remains unclear if the toxicity has any significant influence on N_2 fixation rates, however it appears as though the fundamentally different plankton community in these two mesocosms at high $p\text{CO}_2$, along with deep water addition and dust deposition, created an environment that supported high N_2 fixation rates.

Unicellular diazotrophic cyanobacteria driven dark nitrogen fixation rates

As seen in our *nifH* gene copies, diazotrophs may have particularly benefited from the deep water addition, presumably via the associated PO_4^{3-} and micronutrient supply. There is a chance that seed populations (such as gammaproteobacteria) were introduced into the mesocosms from the deep water as these were undetectable before the deep water addition. Diazotroph abundances were highest in samples from the decay phase. The latter may speak for a standing stock of those diazotrophs, which are able to persist for a certain time even after nutrient drawdown. One of the identified clades, UCYN-B, has been shown to primarily fix N_2 in the dark and C in the light (e.g., Großkopf and LaRoche, 2012; Wilson et al., 2010). However, if this photosynthetic clade is limited by light availability, the highly energy-demanding process of N_2 fixation would have to be sustained by respiration only, thus explaining the lower activity in dark incubations. Dark N_2 fixation rates, however, may be a result of the unicellular cyanobacteria of the UCYN-B clade fixing mainly at night (Mohr et al. 2010b).

Effect of rising carbon dioxide on carbon fixation rates

Previous studies suggest either a positive effect or no significant effect of high $p\text{CO}_2$ on plankton community C fixation rates (e.g., Schulz et al. 2017). Our results from the oligotrophic and eutrophic phases suggest no effect of elevated $p\text{CO}_2$ on phototrophic C fixation. Our C fixation analysis is consistent with the conclusions derived from a ^{14}C based primary production study conducted in the same mesocosm study for the decay phase, when $p\text{CO}_2$ seems to have a positive effect

on C fixation rates (Hernández-Hernández et al. 2018). The magnitude of ^{14}C based C fixation rates during all the phases were comparable to those estimated based on ^{13}C tracer. Assuming photoautotrophs require 1 mol N to fix 6.6 mol C (Redfield 1958), the contribution of N_2 fixation to new nitrogen supply for phototrophic C fixation was moderate (mean value of 4% with highest contribution up to 13%). Dark C fixation rates varied within the analytical uncertainties suggesting absence of lithoautotrophs or chemoautotrophs in our experiments (Figs. 3d, 4d).

Conclusion

Under the applied $p\text{CO}_2$ range (352–1025 μatm), we observed variable effects of elevated $p\text{CO}_2$ on C and N_2 fixation that appeared to depend on nutrient concentrations and bloom status during our 55 day-long experiment. Interestingly, our results suggest positive effect of high $p\text{CO}_2$ on C fixation rates only in the decay phase. The strongest negative effect of CO_2 on N_2 fixation was detected during the oligotrophic phase, prior to the simulated upwelling event. The nutrient-rich deep water and dust deposition had a marked impact on both N_2 fixation and C fixation rates, magnitudes higher than the difference between CO_2 treatments. Our analysis indicated that higher NO_x^- concentrations from addition of deep water in the middle of the study did not inhibit N_2 fixation rates, thus providing more support for challenging the classical paradigm in our understanding of N_2 fixation. Nitrogen fixation in our experiment seems to have responded rather to elevated PO_4^{3-} from deep water (or another nutrient such as Fe from the deep water and dust deposition) despite excess NO_x^- . Preferential consumption of NO_x^- during the growth phase may have amplified the diazotrophic niche in the decay phase. Unicellular diazotrophic cyanobacterium clade UCYN-B seems to have benefited the most from the deep water addition, while gammaproteobacterial abundances might have been introduced to the mesocosms with the deep water addition. We thus conclude that diazotrophic species and N_2 fixation rates respond to elevated $p\text{CO}_2$ in a complex way depending upon nutrient conditions. Our results suggest that N_2 fixation rates can respond positively to enhanced upwelling but after a time-lag of a few days, as diazotrophs may benefit from increased nutrients (PO_4^{3-} and Fe) availability. Coupling of elevated $p\text{CO}_2$ and nutrient exhaustion, as observed in the decay phase and common in the oligotrophic ocean, will also positively impact N_2 fixation rates.

References

- Aure, J., Ø. Strand, S. R. Erga, and T. Strohmeier. 2007. Primary production enhancement by artificial upwelling in a western Norwegian fjord. *Mar. Ecol. Prog. Ser.* **352**: 39–52.
- Badger, M. R., G. D. Price, B. M. Long, and F. J. Woodger. 2005. The environmental plasticity and ecological

- genomics of the cyanobacterial CO₂ concentrating mechanism. *J. Exp. Bot.* **57**: 249–265.
- Barcelos e Ramos, J., H. Biswas, K. G. Schulz, J. LaRoche, and U. Riebesell. 2007. Effect of rising atmospheric carbon dioxide on the marine nitrogen fixer *Trichodesmium*. *Global Biogeochem. Cycles* **21**: GB2028.
- Benavides, M., J. Arístegui, N. S. Agawin, J. L. Cancio, and S. Hernández-León. 2013. Enhancement of nitrogen fixation rates by unicellular diazotrophs vs. *Trichodesmium* after a dust deposition event in the Canary Islands. *Limnol. Oceanogr.* **58**: 267–275.
- Berman-Frank, I., P. Lundgren, Y.-B. Chen, H. Küpper, Z. Kolber, B. Bergman, and P. Falkowski. 2001. Segregation of nitrogen fixation and oxygenic photosynthesis in the marine cyanobacterium *Trichodesmium*. *Science* **294**: 1534–1537.
- Bertilsson, S., O. Berglund, D. M. Karl, and S. W. Chisholm. 2003. Elemental composition of marine *Prochlorococcus* and *Synechococcus*: Implications for the ecological stoichiometry of the sea. *Limnol. Oceanogr.* **48**: 1721–1731.
- Bindoff, N. L., W. W. Cheung, J. G. Kairo, and others. 2019. Changing ocean, marine ecosystems, and dependent communities. In IPCC special report on the ocean and cryosphere in a changing climate. IPCC.
- Bombar, D., R. W. Paerl, R. Anderson, and L. Riemann. 2018. Filtration via conventional glass fiber filters in N¹⁵N₂ tracer assays fails to capture all nitrogen-fixing prokaryotes. *Front. Mar. Sci.* **5**: 6.
- Bonnet, S., T. Moutin, M. Rodier, and others. 2016. Introduction to the project VAHINE: Variability of vertical and trophic transfer of diazotroph derived N in the south west Pacific. *Biogeosciences* **13**: 2803–2814.
- Capone, D. G., J. P. Zehr, H. W. Paerl, B. Bergman, and E. J. Carpenter. 1997. *Trichodesmium*, a globally significant marine cyanobacterium. *Science* **276**: 1221–1229.
- Deutsch, C., J. L. Sarmiento, D. M. Sigman, N. Gruber, and J. P. Dunne. 2007. Spatial coupling of nitrogen inputs and losses in the ocean. *Nature* **445**: 163–167.
- Dickson, A. G., J. Afghan, and G. Anderson. 2003. Reference materials for oceanic CO₂ analysis: A method for the certification of total alkalinity. *Mar. Chem.* **80**: 185–197.
- Doney, S. C., D. S. Busch, S. R. Cooley, and K. J. Kroeker. 2020. The impacts of ocean acidification on marine ecosystems and reliant human communities. *Annu. Rev. Env. Resour.* **45**: 83–112. doi:10.1146/annurev-environ-012320-083019
- Falkowski, P. G. 1997. Evolution of the nitrogen cycle and its influence on the biological sequestration of CO₂ in the ocean. *Nature* **387**: 272–275.
- Fernandez, C., L. Fariás, and O. Ulloa. 2011. Nitrogen fixation in denitrified marine waters. *PLoS One* **6**: e20539.
- Foster, R. A., and J. P. Zehr. 2006. Characterization of diatom–cyanobacteria symbioses on the basis of nifH, hetR and 16S rRNA sequences. *Environ. Microbiol.* **8**: 1913–1925.
- Franz, J., G. Krahmann, G. Lavik, P. Grasse, T. Dittmar, and U. Riebesell. 2012. Dynamics and stoichiometry of nutrients and phytoplankton in waters influenced by the oxygen minimum zone in the eastern tropical Pacific. *Deep Sea Res. Part Oceanogr. Res. Pap.* **62**: 20–31.
- Fu, F.-X., M. R. Mulholland, N. S. Garcia, A. Beck, P. W. Bernhardt, M. E. Warner, S. A. Sanudo-Wilhelmy, and D. A. Hutchins. 2008. Interactions between changing pCO₂, N₂ fixation, and Fe limitation in the marine unicellular cyanobacterium *Crocospaera*. *Limnol. Oceanogr.* **53**: 2472–2484.
- Groszkopf, T., and J. LaRoche. 2012. Direct and indirect costs of dinitrogen fixation in *Crocospaera watsonii* WH8501 and possible implications for the nitrogen cycle. *Front. Microbiol.* **3**: 236.
- Gruber, N., D. Clement, B. R. Carter, and others. 2019. The oceanic sink for anthropogenic CO₂ from 1994 to 2007. *Science* **363**: 1193–1199.
- Hansen, H. P., and F. Koroleff. 2007. Determination of nutrients, p. 159–228. In *Methods of seawater analysis*. Wiley.
- Havenhand, J., S. Dupont, and G. P. Quinn. 2010. Designing ocean acidification experiments to maximise inference. Pp. 67–80 In U. Riebesell, V. J. Fabry, L. Hansson and J. P. Gattuso, eds. *Guide to best practices for ocean acidification research and data reporting*. Publications Office of the European Union, Luxembourg.
- Hernández-Hernández, N., L. T. Bach, M. F. Montero, and others. 2018. High CO₂ under nutrient fertilization increases primary production and biomass in subtropical phytoplankton communities: A mesocosm approach. *Front. Mar. Sci.* **5**: 1–14. doi:10.3389/fmars.2018.00213
- Holl, C. M., and J. P. Montoya. 2005. Interactions between nitrate uptake and nitrogen fixation in continuous cultures of the marine diazotroph *Trichodesmium* (cyanobacteria). *J. Phycol.* **41**: 1178–1183.
- Hutchins, D., F.-X. Fu, Y. Zhang, M. Warner, Y. Feng, K. Portune, P. Bernhardt, and M. Mulholland. 2007. CO₂ control of *Trichodesmium* N₂ fixation, photosynthesis, growth rates, and elemental ratios: Implications for past, present, and future ocean biogeochemistry. *Limnol. Oceanogr.* **52**: 1293–1304.
- Hutchins, D. A., and F. Fu. 2017. Microorganisms and ocean global change. *Nat. Microbiol.* **2**: 17058.
- Inness, A., M. Ades, A. Agusti-Panareda, and others. 2019. The CAMS reanalysis of atmospheric composition. *Atmos. Chem. Phys.* **19**: 3515–3556.
- Jickells, T., E. Buitenhuis, K. Altieri, and others. 2017. A reevaluation of the magnitude and impacts of anthropogenic atmospheric nitrogen inputs on the ocean. *Glob. Biogeochem. Cycles* **31**: 289–305.
- Karl, D. M., and R. M. Letelier. 2008. Nitrogen fixation-enhanced carbon sequestration in low nitrate, low chlorophyll seascapes. *Mar. Ecol. Prog. Ser.* **364**: 257–268.
- Keeling, R. F., and C. D. Keeling. 2017. Atmospheric monthly in situ CO₂ data-mauna loa observatory, Hawaii. Scripps

- CO₂ program data UC San Diego Libr. Digit. Collect. [Accessed 2021 March 22]. doi:[10.6075/J08W3BHW](https://doi.org/10.6075/J08W3BHW)
- Knapp, A. N., J. Dekaezemacker, S. Bonnet, J. A. Sohm, and D. G. Capone. 2012. Sensitivity of *Trichodesmium erythraeum* and *Crocospaera watsonii* abundance and N₂ fixation rates to varying NO₃⁻ and PO₄³⁻ concentrations in batch cultures. *Aquat. Microb. Ecol.* **66**: 223–236.
- Knapp, A. N., K. L. Casciotti, W. M. Berelson, M. G. Prokopenko, and D. G. Capone. 2016. Low rates of nitrogen fixation in eastern tropical South Pacific surface waters. *Proc. Natl. Acad. Sci. USA* **113**: 4398–4403.
- Langlois, R. J., J. LaRoche, and P. A. Raab. 2005. Diazotrophic diversity and distribution in the tropical and subtropical Atlantic Ocean. *Appl. Environ. Microbiol.* **71**: 7910–7919.
- Langlois, R. J., D. Hümmel, and J. LaRoche. 2008. Abundances and distributions of the dominant nifH phylotypes in the northern Atlantic Ocean. *Appl. Environ. Microbiol.* **74**: 1922–1931.
- Law, C. S., E. Breitbarth, L. J. Hoffmann, C. M. McGraw, R. J. Langlois, J. LaRoche, A. Marriner, and K. A. Safi. 2012. No stimulation of nitrogen fixation by non-filamentous diazotrophs under elevated CO₂ in the South Pacific. *Glob. Change Biol.* **18**: 3004–3014.
- Loescher, C. R., T. Großkopf, F. D. Desai, and others. 2014. Facets of diazotrophy in the oxygen minimum zone waters off Peru. *ISME J.* **8**: 2180–2192.
- Lomas, M. W., A. Burke, D. Lomas, D. Bell, C. Shen, S. T. Dyhrman, and J. W. Ammerman. 2010. Sargasso Sea phosphorus biogeochemistry: An important role for dissolved organic phosphorus (DOP). *Biogeosciences* **7**: 695–710.
- Lueker, T. J., A. G. Dickson, and C. D. Keeling. 2000. Ocean pCO₂ calculated from dissolved inorganic carbon, alkalinity, and equations for K₁ and K₂: Validation based on laboratory measurements of CO₂ in gas and seawater at equilibrium. *Mar. Chem.* **70**: 105–119.
- Mills, M. M., and K. R. Arrigo. 2010. Magnitude of oceanic nitrogen fixation influenced by the nutrient uptake ratio of phytoplankton. *Nat. Geosci.* **3**: 412–416.
- Mills, M. M., C. Ridame, M. Davey, J. la Roche, and R. J. Geider. 2004. Iron and phosphorus co-limit nitrogen fixation in the eastern tropical North Atlantic. *Nature* **429**: 292–294.
- Mohr, W., T. Grosskopf, D. W. Wallace, and J. LaRoche. 2010a. Methodological underestimation of oceanic nitrogen fixation rates. *PLoS One* **5**: e12583.
- Mohr, W., M. P. Intermaggio, and J. LaRoche. 2010b. Diel rhythm of nitrogen and carbon metabolism in the unicellular, diazotrophic cyanobacterium *Crocospaera watsonii* WH8501. *Environ. Microbiol.* **12**: 412–421.
- Montoya, J. P., M. Voss, P. Kähler, and D. G. Capone. 1996. A simple, high-precision, high-sensitivity tracer assay for N₂ fixation. *Appl. Environ. Microbiol.* **62**: 986–993.
- Montoya, J. P., E. J. Carpenter, and D. G. Capone. 2002. Nitrogen fixation and nitrogen isotope abundances in zooplankton of the oligotrophic North Atlantic. *Limnol. Oceanogr.* **47**: 1617–1628.
- Moss, R. H., J. A. Edmonds, K. A. Hibbard, and others. 2010. The next generation of scenarios for climate change research and assessment. *Nature* **463**: 747–756.
- Narayan, N., A. Paul, S. Mulitza, and M. Schulz. 2010. Trends in coastal upwelling intensity during the late 20th century. *Ocean Sci.* **6**: 815–823.
- Paul, A. J., L. T. Bach, K.-G. Schulz, and others. 2015. Effect of elevated CO₂ on organic matter pools and fluxes in a summer Baltic Sea plankton community. *Biogeosciences* **12**: 6181–6203.
- Pierrot, D., D. Wallace, E. Lewis, and others. 2011. MS Excel program developed for CO₂ system calculations.
- Rabouille, S., G. S. Cabral, and M. L. Pedrotti. 2017. Towards a carbon budget of the diazotrophic cyanobacterium *Crocospaera*: Effect of irradiance. *Mar. Ecol. Prog. Ser.* **570**: 29–40.
- Redfield, A. C. 1958. The biological control of chemical factors in the environment. *Am. Sci.* **46**: 230A–221A.
- Riebesell, U. 2004. Effects of CO₂ enrichment on marine phytoplankton. *J. Oceanogr.* **60**: 719–729.
- Riebesell, U., J. Czerny, K. von Bröckel, and others. 2013. A mobile sea-going mesocosm system—new opportunities for ocean change research. *Biogeosciences* **10**: 1835–1847.
- Riebesell, U., N. Aberle-Malzahn, E. P. Achterberg, and others. 2018. Toxic algal bloom induced by ocean acidification disrupts the pelagic food web. *Nat. Clim. Change* **8**: 1082–1086.
- Sangrà, P., C. Troupin, B. Barreiro-González, E. Desmond Barton, A. Orbi, and J. Arístegui. 2015. The cape Ghir filament system in August 2009 (NW Africa). *J. Geophys. Res. Oceans* **120**: 4516–4533.
- Santana-Falcón, Y., E. Mason, and J. Arístegui. 2020. Offshore transport of organic carbon by upwelling filaments in the canary current system. *Prog. Oceanogr.* **186**: 102322.
- Schulz, K. G., L. T. Bach, R. G. Bellerby, and others. 2017. Phytoplankton blooms at increasing levels of atmospheric carbon dioxide: Experimental evidence for negative effects on prymnesiophytes and positive on small picoeukaryotes. *Front. Mar. Sci.* **4**: 64.
- Singh, A., S. Baer, U. Riebesell, A. Martiny, and M. Lomas. 2015. C:N:P stoichiometry at the Bermuda Atlantic time-series study station in the North Atlantic Ocean. *Biogeosciences* **12**: 6389–6403.
- Singh, A., L. T. Bach, T. Fischer, and others. 2017. Niche construction by non-diazotrophs for N₂ fixers in the eastern tropical North Atlantic Ocean. *Geophys. Res. Lett.* **44**: 6904–6913.
- Slawyk, G., Y. Collos, and J. Auclair. 1977. The use of the ¹³C and ¹⁵N isotopes for the simultaneous measurement of carbon and nitrogen turnover rates in marine phytoplankton. *Limnol. Oceanogr.* **22**: 925–932. doi:[10.4319/lo.1977.22.5.0925](https://doi.org/10.4319/lo.1977.22.5.0925)

- Tang, W., S. Wang, D. Fonseca-Batista, and others. 2019. Revisiting the distribution of oceanic N₂ fixation and estimating diazotrophic contribution to marine production. *Nat. Commun.* **10**: 1–10.
- Taucher, J., L. T. Bach, T. Boxhammer, and others. 2017. Influence of ocean acidification and deep water upwelling on oligotrophic plankton communities in the subtropical North Atlantic: Insights from an in situ Mesocosm study. *Front. Mar. Sci.* **4**: 85.
- Taucher, J., J. Aristegui, L. T. Bach, W. Guan, M. F. Montero, A. Nauendorf, E. P. Achterberg, and U. Riebesell. 2018a. Response of subtropical phytoplankton communities to ocean acidification under oligotrophic conditions and during nutrient fertilization. *Front. Mar. Sci.* **5**: 330.
- Taucher, J., P. Stange, M. Algueró-Muñiz, L. T. Bach, A. Nauendorf, R. Kolzenburg, J. Büdenbender, and U. Riebesell. 2018b. In situ camera observations reveal major role of zooplankton in modulating marine snow formation during an upwelling-induced plankton bloom. *Prog. Oceanogr.* **164**: 75–88.
- Thompson, A. W., and J. P. Zehr. 2013. Cellular interactions: Lessons from the nitrogen-fixing cyanobacteria. *J. Phycol.* **49**: 1024–1035.
- Thompson, A. W., R. A. Foster, A. Krupke, B. J. Carter, N. Musat, D. Vaultot, M. M. Kuypers, and J. P. Zehr. 2012. Unicellular cyanobacterium symbiotic with a single-celled eukaryotic alga. *Science* **337**: 1546–1550.
- Tyrrell, T. 1999. The relative influences of nitrogen and phosphorus on oceanic primary production. *Nature* **400**: 525–531.
- Wang, D., T. C. Gouhier, B. A. Menge, and A. R. Ganguly. 2015. Intensification and spatial homogenization of coastal upwelling under climate change. *Nature* **518**: 390–394.
- Wannicke, N., C. Frey, C. S. Law, and M. Voss. 2018. The response of the marine nitrogen cycle to ocean acidification. *Glob. Change Biol.* **24**: 5031–5043.
- Weiss, R. F. 1970. The solubility of nitrogen, oxygen and argon in water and seawater. *Proc Deep Sea Res Oceanogr Abstr.* **17**: 721–735.
- Wilson, S. T., R. A. Foster, J. P. Zehr, and D. M. Karl. 2010. Hydrogen production by *Trichodesmium erythraeum* *Cyanothece* sp. and *Crocospaera watsonii*. *Aquat. Microb. Ecol.* **59**: 197–206.
- Xiu, P., F. Chai, E. N. Curchitser, and F. S. Castruccio. 2018. Future changes in coastal upwelling ecosystems with global warming: The case of the California current system. *Sci. Rep.* **8**: 2866.
- Zani, S., M. T. Mellon, J. L. Collier, and J. P. Zehr. 2000. Expression of nifH genes in natural microbial assemblages in Lake George, New York, detected by reverse transcriptase PCR. *Appl. Environ. Microbiol.* **66**: 3119–3124.
- Zehr, J. P., and D. G. Capone. 2020. Changing perspectives in marine nitrogen fixation. *Science* **368**: eaay9514.
- Zehr, J. P., S. R. Bench, B. J. Carter, I. Hewson, F. Niazi, T. Shi, H. J. Tripp, and J. P. Affourtit. 2008. Globally distributed uncultivated oceanic N₂-fixing cyanobacteria lack oxygenic photosystem II. *Science* **322**: 1110–1112.
- Zhang, X., B. B. Ward, and D. M. Sigman. 2020. Global nitrogen cycle: Critical enzymes, organisms, and processes for nitrogen budgets and dynamics. *Chem. Rev.* **120**: 5308–5351.

Acknowledgments

Plataforma Oceánica de Canarias (PLOCAN) and Spanish Bank of Algae are acknowledged for sharing its research facilities with us to facilitate our experiments. RV *Hesperides* team is thanked for deploying and recovering the mesocosms. We thank the KOSMOS team for their immense help in sampling the mesocosms; Andrea Ludwig is particularly appreciated for coordinating the campaign logistics. We thank Kerstin Nachtigall for IRMS analysis and Mario Esposito for nutrient analysis. We acknowledge the use of the CAMS reanalysis data available from the ECMWF, UK. This project was funded by the German Federal Ministry of Education and Research (BMBF) in the framework of the coordinated project BIOACID—Biological Impacts of Ocean Acidification, phase 2 (FKZ 03F06550). Arvind Singh was financially supported by a grant (CP1213) from the Cluster of Excellence 80 “The Future Ocean.” Arvind Singh received additional funding from the Leibniz Award 2012 (awarded to Ulf Riebesell) by the German Research Foundation (DFG). Carolin R. Löscher was funded by the EU’s Horizon 2020 program (NITROX, Grant #704272) and by the Villum Foundation (Grants #16518 and #29411). Two anonymous reviewers are thanked for their constructive comments.

Conflict of interest

None declared.

Submitted 12 August 2020

Revised 20 November 2020

Accepted 02 May 2021

Associate editor: Ilana Berman-Frank